

Surface energetics and growth of pentacene

John E. Northrup

Palo Alto Research Center, 3333 Coyote Hill Road, Palo Alto, California 94304

Murilo L. Tiago and Steven G. Louie

*Department of Physics, University of California at Berkeley, Berkeley, California 94720**and Materials Science Division, Lawrence Berkeley National Laboratory, Berkeley, California 94720*

(Received 12 June 2002; published 27 September 2002)

First-principles pseudopotential density-functional calculations for pentacene and anthracene are used to obtain atomic structures, cohesive energies, and surface energies for the low index surfaces. For pentacene, calculations predict that the (001) surface has a much lower surface energy than the other surfaces. From the first-principles results a general model of the intermolecular bonding is developed. This model may be employed to estimate the surface energies and cohesive energy for *any* polyacene crystal. Implications of the present results for understanding the temperature dependence of the growth morphology of pentacene are discussed.

DOI: 10.1103/PhysRevB.66.121404

PACS number(s): 68.35.Md, 61.66.Hq

There is a substantial interest in organic semiconductors such as pentacene and other polyacenes because of the high mobilities exhibited by single crystals¹ and because of the potential to employ thin-film depositions of these materials to fabricate electronic devices.^{2–5} Room-temperature mobilities in the range of $1 \text{ cm}^2/\text{V s}$ can be achieved in pentacene thin-film transistors,^{3–5} making this material a possible alternative to amorphous silicon. The possibility that grain boundaries formed during growth may limit the mobility has motivated experimental studies of the growth morphology as well as attempts to increase the grain size by modifying the interaction between the molecule and the substrate.^{6,7} An improved understanding of thin-film growth would be enabled by knowledge of the intermolecular bonding energetics and its anisotropy. This requirement has motivated the present first-principles calculations of the surface energies of pentacene ($\text{C}_{22}\text{H}_{14}$) and anthracene ($\text{C}_{14}\text{H}_{10}$).

Experimental studies of the morphology of evaporated pentacene films on various substrates indicate that the crystals tend to be oriented so that the (001) face is parallel to the substrate.^{2,8,9} It is shown here that the (001) surface of pentacene has a much lower surface energy than other low index surfaces, and that the bonds between molecules in the same layer are several times stronger than those between molecules in adjacent layers. This anisotropy in the bonding is the driving force for the film to exhibit (001) orientation when deposited on a substrate with which it interacts weakly.

Total-energy calculations were performed within the local density-functional theory using first-principles pseudopotentials and the Ceperley-Alder exchange correlation-energy functional. Details of the method are discussed elsewhere.^{10,11} A plane-wave basis with a cutoff energy of 40 Ry is employed. With this cutoff, the binding energy of bulk pentacene with respect to isolated pentacene molecules is converged adequately: Increasing the plane-wave cutoff from 40 to 60 Ry led to a negligible change in the molecular cohesive energy of about 0.02 eV.

Pentacene can exhibit several different polytypes corresponding to different packing arrangements of the $\text{C}_{22}\text{H}_{14}$

molecules.¹² The calculations reported here were performed for the triclinic structure determined by Campbell *et al.*,^{13,14} using *x*-ray diffraction. The lattice vectors determined in that study are Robertson, and Trotter $\mathbf{a} = a(0.9973, 0.0732, 0)$, $\mathbf{b} = b(0, 1, 0)$, and $\mathbf{c} = c(-0.36974, -0.2062, 0.9056)$. The lengths of the vectors are $a = 7.90 \text{ \AA}$, $b = 6.06 \text{ \AA}$ and $c = 16.01 \text{ \AA}$. The angle between \mathbf{a} and \mathbf{b} is 85.8° , that between \mathbf{b} and \mathbf{c} is 101.9° , and that between \mathbf{a} and \mathbf{c} is 112.6° . These lattice parameters were kept fixed during the optimization of the internal coordinates of the C and H atoms.

Shown in Fig. 1 is a schematic representation of a single pentacene molecule. To form the bulk phase these molecules are arranged in a herringbone pattern with molecules centered at (0 0 0) and (1/2 1/2 0). Pentacene forms a layered structure with a separation between adjacent layers of 14.5 Å in the *z* direction. Figure 2 depicts a single layer of pentacene in the *a*-*b* plane. There are two molecules in each cell, and they are oriented so that their respective longitudinal axes, defined as *L* in Fig. 1, form angles of 22.2° and 20.4° with respect to the *z* axis. Each molecule is approximately planar, and the calculations indicate that the maximum deviation from planarity of each molecule is less than 0.02 Å. The calculated C—C bonds vary in length from 1.35 to 1.44 Å and are in excellent agreement with experimental values. A comparison between the experimental and theoretical values is given in Table I. The intermolecular bonding in pentacene is a result of dipole-dipole and weak van der Waals interac-

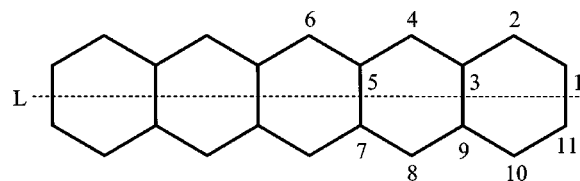


FIG. 1. A single pentacene molecule ($\text{C}_{22}\text{H}_{14}$) consists of five benzene rings. Each C atom is threefold coordinated. The H atoms are not shown. The calculated C—H bonds have length $\sim 1.096 \text{ \AA}$. The calculated bond distances between C atoms are listed in Table I. The dashed line *L* defines the longitudinal axis of the molecule.

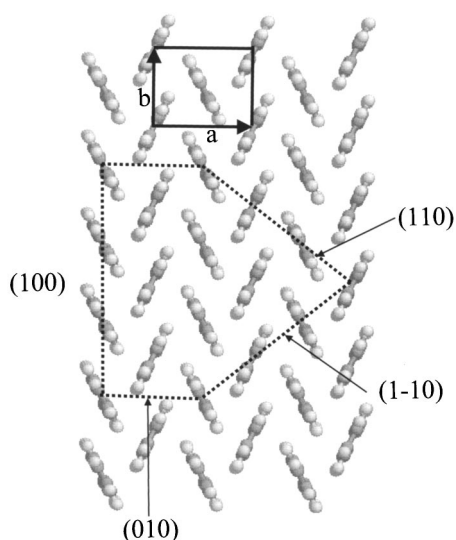


FIG. 2. A single **a-b** layer of pentacene is depicted. The unit cell of the crystal contains two pentacene molecules. The longitudinal axes of the two molecules form angles of $(104.5^\circ, 106.4^\circ, 22.2^\circ)$ and $(104.5^\circ, 104.0^\circ, 20.4^\circ)$ with respect to the x , y , and z axis. One is viewing the **a-b** layer along the longitudinal axis of a molecule.

tions. As the molecules are brought together the molecular π orbitals of the isolated molecules broaden into bands of width ~ 0.5 eV.¹⁵

Another form of pentacene has been reported by Siegrist *et al.*¹⁶ This polymorph also adopts a triclinic structure, but the lattice vectors and angles between the axes differ from those of the Campbell form. Nevertheless, our calculations predict that the cohesive energies of the Siegrist structure and the Campbell structure differ by only about 0.05 eV/molecule. Because both types of structures exhibit the same kind of herringbone arrangement of the molecules within the **a-b** plane, one expects the surface energies of the two polymorphs to be similar.

One may define a *molecular cohesive energy* (E_{coh}) for an organic crystal to be the energy reduction arising from bringing isolated molecules together to form a crystal. The molecular cohesive energy for pentacene is found to be 1.3 eV per molecule. It is clear from this result that pentacene molecules are bound together more weakly than the atoms in typical inorganic crystals where the cohesive energies (rela-

TABLE I. Comparison between calculated and experimental bond distances. The experimental values are from Ref. 14.

C—C bonds (pentacene)	Theory (\AA)	Experiment (\AA)
1–2	1.350	1.35
2–3	1.413	1.42
3–4	1.373	1.38
4–5	1.394	1.40
5–6	1.384	1.39
1–11	1.412	1.43
3–9	1.439	1.44
5–7	1.443	1.45

TABLE II. Surface energies of pentacene.

Pentacene surface	$E_{\text{form}}/\text{cell}$ (eV)	γ ($\text{meV}/\text{\AA}^2$)	Model
(001)	0.15	3.1	0.15
(100)	0.45	4.8	0.45
(110)	0.71	4.7	0.75
(1–10)	0.72	4.8	0.75
(010)	0.75	6.4	0.75

tive to isolated atoms) are typically between 4 and 5 eV per atom. For this reason growth of pentacene crystals must take place at lower temperatures than those employed in the growth of inorganic semiconductors. Typical growth temperatures for pentacene are less than 100°C .

Surface energies were calculated for the (001), (100), (010), (110), and (1-10) surfaces. These surfaces are indicated schematically in Fig. 2. The surface energy calculations were performed using a repeated slab geometry with four molecules per cell and a vacuum separation between surfaces that is large enough to remove the interaction between the surfaces. Increasing the vacuum separation between (010) surfaces from 15 to 19 bohrs led to a negligible change in surface energy of less than 0.01 eV/cell. The calculated energies are listed in Table II. Based on the facets considered in this work, an equilibrium crystal shape (ECS) has been constructed and is depicted in Fig. 3. The (001) surface is found to be the lowest in energy, having a formation energy of 0.15 eV per surface unit cell. This translates into a surface energy, γ , of $3.1 \text{ meV}/\text{\AA}^2$, a value that is much lower than the surface energies for inorganic semiconductors, where values are higher typically by a factor ~ 30 . The very low values of the surface energies for pentacene result from the fact that no covalent bonds must be broken to create surfaces. The (010) surface of pentacene has a formation energy of 0.75 eV/cell, corresponding to $\gamma = 6.4 \text{ meV}/\text{\AA}^2$. Of the surface orientations for which we have performed calculations, the (010) facet has the highest surface energy, and in fact this facet would be absent from the ECS.

The calculated surface energies may be employed to determine the parameters of a model by which one may deter-

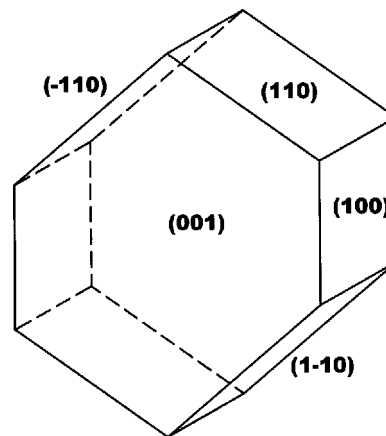


FIG. 3. The equilibrium crystal shape of pentacene was determined from the calculations discussed in the text.

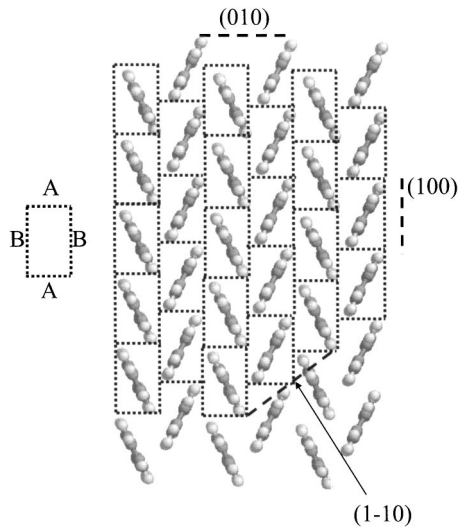


FIG. 4. A single **a-b** layer of pentacene is divided into rectangular cells with sides A and B . Intermolecular interactions across side A have a cumulative strength $A=0.3$ eV. Intermolecular interactions across side B have cumulative strength $B=0.9$ eV as discussed in the text.

mine, for any polyacene, surface energies, cohesive energies, and binding energies of adsorbed molecules on different facets. To do this we define an orientation dependent effective bond strength between pentacene molecules. As shown in Fig. 4, the crystal is partitioned into cells and it is postulated that each molecule forms bonds with its neighbors of strength A or B depending on the orientation. Bonds across the short side of the cell have strength A and bonds across the longer side of the cell have strength B . Then, to cleave the crystal along any particular plane, one must break certain numbers of A -type and B -type bonds, and one can express the surface energy of any plane in terms of the energy cost to break these bonds. Thus the surface energy per surface unit cell of the (100) surface is equal to $B/2$, and the surface energy per surface unit cell of the (010) surface is $(2A+B)/2$. From these two relations the pentacene effective bond strengths are determined: $A=0.3$ eV and $B=0.9$ eV. A third effective bond strength is determined by the surface energy per cell of the (001) surface and is $C=0.15$ eV. The predictive value of this model may be tested in two ways. First, note that the model predicts the energies of the (1-10) and (110) surfaces to be the same and to be equal to $(2A+B)/2=0.75$ eV/cell. This is in excellent agreement with the values determined in the first-principles calculations of 0.72 eV/cell and 0.71 eV/cell. Second, the model predicts the cohesive energy of the crystal to be $A+B+C$, which is 1.35 eV. This is in excellent agreement with the calculated value of 1.3 eV and shows that only $C/(A+B+C)\sim 10\%$ of the cohesive energy results from the bonds between neighboring layers.

As will be discussed below, this model may be employed to estimate the energy of any surface of pentacene, and also the binding energies of molecules on these surfaces. However, before turning to that discussion we argue that the model can be generalized to the other polyacenes, such as

TABLE III. Surface energies of anthracene.

Anthracene	$E_{\text{form}}/\text{cell}$ (eV)	γ (meV/Å ²)	Model
(001)	0.17	3.3	0.15
(010)	0.45	5.7	0.45
(100)	0.28	4.1	0.27

naphthalene, anthracene, tetracene, and hexacene. To make this argument we need to know the cohesive energy and surface energies for anthracene.

Anthracene is constructed from three benzene rings and exhibits a herringbone molecular packing that is similar to pentacene. The structure of anthracene is monoclinic with $a=8.562$ Å, $b=6.038$ Å, $c=11.184$ Å and $\beta=124.5^\circ$.¹⁷ First-principles calculations of the cohesive energy and the surface energies for anthracene are summarized in Table III. The calculated cohesive energy is 0.83 eV/molecule, the formation energy of the (001) surface is 0.17 eV/cell, the energy of the (010) surface is 0.45 eV/cell and the energy of the (100) surface is 0.28 eV/cell. The corresponding surface energies are 3.3, 5.7, and 4.1 meV/Å². As for pentacene the (001) surface has a lower surface energy than (100) and (010), but the anisotropy is slightly less than for pentacene.

Now, it is possible to relate the surface formation energies for anthracene to those obtained for pentacene via a simple scaling relation. Define effective bond strengths A_n , B_n , and C_n for a polyacene having n benzene rings per molecule ($n=5$ for pentacene and $n=3$ for anthracene). It is proposed that A_n and B_n scale as the number of benzene rings, but that C_n is independent of the number of rings, so that $A_3=3/5 A_5$ and $B_3=3/5 B_5$. In this model the cohesive energy of anthracene is $E_{\text{coh}}(\text{anthracene})=C_3+A_3+B_3=C+3/5(A+B)=0.87$ eV. This is in good agreement with the value obtained in first-principles calculations, 0.83 eV/molecule. Likewise the surface energies for the (100) and (010) faces may be estimated using this model. The values obtained in first-principles calculations for anthracene and those obtained via the model are compared in Table III. The agreement is excellent. It is therefore proposed that the model may be applied also to calculate the corresponding quantities in other polyacene materials. In particular, it should be possible to express the cohesive energy for a polyacene in terms of the number of benzene rings as $E_{\text{coh}}(n)=\lambda+\beta n$ where $\lambda\sim 0.15$ eV and $\beta\sim 0.24$ eV. For anthracene the molecular cohesive energy has been determined experimentally¹⁸ to be approximately 1.0 eV. Our result is in good agreement with this value.

This simple model of the intermolecular bonding may also be employed to estimate the binding energies of molecules on various surfaces relative to isolated molecules. To do this we make the simplifying assumption that the structural change produced by molecular binding corresponds to a simple continuation of the bulk crystal lattice. It should then be clear from an examination of Fig. 4 that the molecular binding energies on the various surfaces are as follows: $E_b(100)=B=0.9$ eV, $E_b(010)=A+B=1.2$ eV, and $E_b(110)=E_b(1-10)=A+B/2=0.75$ eV. The same assumption gives $E_b(001)=C=0.15$ eV. The binding energy of a

molecule at a step on the (001) surface [relative to its energy on the (001) terrace] should be quite similar to the binding energy on the corresponding surfaces. Therefore, the binding energies to steps on the (001) surface are predicted to lie in the range from 0.75 to 1.2 eV.

We may exploit this model of the energetics to gain some insight into growth of pentacene from the vapor. It has been shown experimentally that growth of pentacene at $T_g = 25^\circ\text{C}$ may be described in terms of a diffusion-limited aggregation model in which the pentacene molecule is assumed to become immobilized once it has diffused to a step edge.⁵ The values obtained here for the binding energies of molecules to the various surfaces seem large enough to support that assumption. For example, the binding energy of a molecule attached to the (100) facet is $\sim 36kT_g$ (0.9 eV) in these low-temperature growth conditions. This corresponds to a Boltzmann factor for detachment of $\exp(-E/kT) = 10^{-16}$. To estimate the residence time we assume an attempt frequency for detachment of $\nu = 2 \times 10^{12}$ Hz. This corresponds to the energy (8.5 meV) measured¹ for a phonon mode corresponding to intermolecular vibration. The residence time is defined as $\nu^{-1} \exp(E/kT)$. In this way one arrives at an estimated residence time of a molecule at the (100) step of 2×10^3 sec for $T_g = 25^\circ\text{C}$. On the other hand, in studies of growth carried out at somewhat higher temperatures ($T_g \sim 100^\circ\text{C}$) steps with (1-10) and (110) orientation have been observed.⁸ These latter studies suggest that for $T_g \sim 100^\circ\text{C}$ some degree of transport can occur between different step facets, and so the growth velocity of steps becomes orientation dependent. At this higher temperature the binding energy to the (100) surface is $\sim 29kT_g$ and the corresponding Boltzmann factor is increased by about three orders of magnitude. For $T_g = 100^\circ\text{C}$ the estimated residence time of a molecule bound to a (100) step is on the order of one second. Since the typical deposition time is 10 to 30 sec/layer,^{8,9} it is plausible that the molecule can attach and detach from several steps before incorporating during growth at $T_g = 100^\circ\text{C}$. However, at $T_g = 25^\circ\text{C}$ the molecule is likely to remain attached at the step to which it first binds. This argument is qualitative, of course, but it does indicate that the growth morphology of pentacene can change significantly between 25°C and 100°C . It is also interesting to note

TABLE IV. Estimated energies of steps on the (001) pentacene surface.

Step normal	Step facet	Step energy	Energy (meV/Å)
a	(100)	$E_{\text{form}}(100)/b$	75
a + b	(110)	$E_{\text{form}}(110)/ \mathbf{a} - \mathbf{b} $	74
a - b	(1-10)	$E_{\text{form}}(110)/ \mathbf{a} + \mathbf{b} $	70
b	(010)	$E_{\text{form}}(100)/a$	95

that according to this model the (110) and (1-10) facets are those for which the binding energies are expected to be lowest in comparison to the other in-plane facets. This result could explain why the growth velocity of the (110) and (1-10) steps would be relatively slow in comparison to the (010) and (100) steps, and why these facets are seen in the films studied in Ref. 8.

The energies associated with creating monolayer height steps on the (001) surface result from breaking *A*- and *B*-type bonds in the **a-b** plane, and the model may be employed to make estimates of the step energies. The energy cost of creating a step is the additional surface energy created per unit length by the step. The step energies obtained in this way vary from 70 to 95 meV/Å and are given in Table IV. The (110) and (1-10) oriented steps have the lowest energies.

In summary, first-principles pseudopotential density-functional total-energy calculations have been employed to determine the cohesive and surface energies for pentacene and anthracene. In each case the (001) surface exhibits the lowest surface energy. A model of the intermolecular bonding in these types of polyacenes enables estimates to be made for the various surface energies and cohesive energies for the entire class of polyacenes. Estimates of the binding energies of molecules on different surfaces and at steps can be made using this model. These energies provide insight into the temperature dependence of growth morphology observed experimentally.

Work in Berkeley was supported by the National Science Foundation Grant No. DMR00-87088 and by the Director, Office of Science, Office of Basic Energy Sciences, Division of Materials Science and Engineering, U.S. Department of Energy under Contract No. DE-AC03-76SF00098.

¹J. H. Schon *et al.*, Phys. Rev. Lett. **86**, 3843 (2001).

²C. D. Dimitrakopoulos *et al.*, J. Appl. Phys. **80**, 2501 (1996).

³S. F. Nelson *et al.*, Appl. Phys. Lett. **72**, 1854 (1998).

⁴C. D. Dimitrakopoulos *et al.*, Science **283**, 822 (1999).

⁵R. A. Street *et al.*, Appl. Phys. Lett. **80**, 1658 (2002).

⁶Frank-J. Meyer zu Heringdorf *et al.*, Nature (London) **412**, 517 (2001).

⁷I. Kymissis *et al.*, IEEE Trans. Electron Devices **48**, 1060 (2001).

⁸I. P. M. Bouchoms *et al.*, Synth. Met. **104**, 175 (1999).

⁹D. Knipp *et al.*, Proc. SPIE **3366**, 8 (2001).

¹⁰R. Stumpf and M. Scheffler, Comput. Phys. Commun. **79**, 447

(1994).

¹¹J. E. Northrup and J. Neugebauer, Phys. Rev. B **52**, 17 001 (1995).

¹²E. Venuti *et al.*, J. Am. Chem. Soc. **124**, 2128 (2002).

¹³R. B. Campbell *et al.*, Acta Crystallogr. **14**, 705 (1961).

¹⁴R. B. Campbell *et al.*, Acta Crystallogr. **15**, 289 (1962).

¹⁵M. L. Tiago *et al.*, (unpublished).

¹⁶T. Siegrist *et al.*, Angew. Chem. Int. Ed. Engl. **40**, 1732 (2001).

¹⁷R. W. G. Wyckoff, *Crystal Structures* (Wiley, New York, 1964).

¹⁸H. Inokuchi and H. Akamatu, Solid State Phys. **12**, 93 (1961); L. Malaspina *et al.*, J. Chem. Phys. **59**, 387 (1973).